Research Article | Vol. 26, No. 19 | 17 Sep 2018 | OPTICS EXPRESS 24723

Optics EXPRESS

kW-class fiber-coupled diode laser source based on dense spectral multiplexing of an ultra-narrow channel spacing

HONGBO ZHU, XINGCHEN LIN, YAWEI ZHANG, JIANWEI ZHANG, BIAO WANG, JINLONG ZHANG, LI QIN, YONGQIANG NING, AND HAO WU*

Changchun Institute of Optics, Fine Mechanics and Physics, Chinese Academy of Sciences, No.3888, Nanhu Road, Changchun 130033, China

*vicz365@163.com

Abstract: A dense spectral multiplexing structure based on the reflective volume Bragg gratings is introduced to realize the diode laser multiplexing with an ultra-narrow channel spacing of 1.5 nm. With the combination of polarization multiplexing and coarse spectral multiplexing, a diode laser source producing 2045 W power from an output fiber with a core diameter of 105 μm and NA of 0.2 is achieved at an injection current of 10 A. The electro-optical and optical-optical efficiency of the laser source is 42% and 76%, respectively. Experimental results demonstrate the ability of dense spectral multiplexing based on VBG to realize high output power and brightness.

OCIS codes: (140.2020) Diode lasers; (090.7330) Volume gratings; (140.3298) Laser beam combining; (060.4230) Multiplexing; (140.5960) Semiconductor lasers; (140.3460) Lasers.

References and links

1. R. K. Huang, B. Chann, and J. D. Glenn, "Ultra-high brightness, wavelength-stabilized, kW-class fiber coupled diode laser," Proc. SPIE **7918**, 791810 (2011).
2. J. A. Alcock and B. Baufeld, "Diode laser welding of stainless steel 304L," J. Mater. Process. Technol. **240**, 138–144 (2017).
3. G. C. Rodrigues, J. Pencinovsky, M. Cuypers, and J. R. Duflou, "Theoretical and experimental aspects of laser cutting with a direct diode laser," Opt. Lasers Eng. **61**, 31–38 (2014).
4. A. Sevian, O. Andrusyak, I. Ciapurin, V. Smirnov, G. Venus, and L. Glebov, "Efficient power scaling of laser radiation by spectral beam combining," Opt. Lett. **33**(4), 384–386 (2008).
5. H. B. Zhu, M. M. Hao, J. W. Zhang, W. Y. Ji, X. C. Lin, J. S. Zhang, and Y. Q. Ning, "Development and thermal management of 10 kW CW, direct diode laser source," Opt. Laser Technol. **76**, 101–105 (2016).
6. S. Ried, S. Rauch, L. Irmler, J. Rikels, A. Killi, E. Papastathopoulos, E. Sarailou, and H. Zimer, "Next generation diode laser with enhanced brightness," Proc. SPIE **10514**, 105140G (2018).
7. R. K. Huang, B. Chann, J. Burgess, B. Lochman, W. Zhou, M. Cruz, R. Cook, D. Dugmore, J. Shattuck, and P. Tayebati, "TeraDiode's high brightness semiconductor lasers," Proc. SPIE **9730**, 97300C (2016).
8. S. Heinemann, H. Fritsche, B. Kruschke, T. Schmidt, and W. Gries, "Compact high brightness diode laser emitting 500 W from a 100 μm fiber," Proc. SPIE **8605**, 86050Q (2013).
9. U. Witte, F. Schneider, M. Traub, D. Hoffmann, S. Drovs, T. Brand, and A. Unger, "kW-class direct diode laser for sheet metal cutting based on DWDM of pump modules by use of ultra-steep dielectric filters," Opt. Express **24**(20), 22917–22929 (2016).
10. U. Witte, M. Traub, A. D. Meo, M. Hamann, D. Rubel, S. Hengesbach, and D. Hoffmann, "Compact 35 μm fiber coupled diode laser module based on dense wavelength division multiplexing of NBA mini-bars," Proc. SPIE **9733**, 97330H (2016).
11. S. Hengesbach, S. Klein, M. Traub, and U. Witte, "Simultaneous frequency stabilization, wavelength multiplexing and improvement of beam quality using a self-optimizing external cavity diode laser," Opt. Lett. **41**(3), 595–598 (2016).
12. S. Hengesbach, U. Witte, M. Traub, and D. Hoffmann, "Design of a DFB/DBR Ddiode Llaser Mmodule including spectral multiplexing based on VBGs," Proceedings of IEEE Conference on High Power Diode Lasers & Systems Conference, 16–17 (2014).
13. P. Leisher, M. Reynolds, A. Brown, K. Kennedy, L. Bao, J. Wang, M. Grimshaw, M. DeVito, S. Karlsen, J. Small, C. Ebert, R. Martinsen, and J. Haden, "Reliability of high power diode laser systems based on single emitters," Proc. SPIE **7918**, 791802 (2011).
14. K. Price, S. Karlsen, P. Leisher, and R. Martinsen, "High brightness fiber coupled pump laser development," Proc. SPIE **7583**, 758308 (2015).

#323010 https://doi.org/10.1364/OE.26.024723
Journal © 2018 Received 14 Feb 2018; revised 10 May 2018; accepted 12 May 2018; published 6 Sep 2018

15. R. Liu, X. C. Jiang, T. Yang, X. G. He, Y. Y. Gao, J. Zhu, T. J. Zhang, W. R. Guo, B. H. Wang, Z. J. Guo, L. Y. Zhang, and L. Chen, "High- brightness 9xx nm fiber coupled diode lasers," Proc. SPIE **9348**, 93480V (2015).
16. H. An, Y. Xiong, C.-L. J. Jiang, B. Schmidt, and G. Treusch, "Methods for slow axis beam quality improvement of high power broad area diode lasers," Proc. SPIE **8965**, 89650U (2014).
17. A. Sevian, O. Andrusyak, I. Ciapurin, G. Venus, and L. Glebov, "Spectral beam combining with volume Bragg gratings: Cross-talk analysis and optimization schemes," Proc. SPIE **6216**, 62160V (2006).
18. O. Andrusyaka, V. Smirnovb, G. Venusa, N. Vorobieva, and L. Glebov, "Applications of volume Bragg gratings for spectral control and beam combining of high power fiber lasers," Proc. SPIE **7195**, 71951Q (2009).
19. S. Hengesbach, N. Krauch, C. Holly, and U. Martin Traub, "Witte, and Dieter Hoffmann, "High-power dense wavelength division multiplexing of multimode diode laser radiation based on volume Bragg grating," Opt. Lett. **38**(4), 3154–3157 (2013).
20. S. Hengesbach, C. Holly, N. Krauch, U. Witte, T. Westphalen, M. Traub, and D. Hoffmann, "High-Power Dense Wavelength Division Multiplexing (HP-DWDM) of frequency stabilized 9xx diode laser bars with a channel spacing of 1.5 nm," Proc. SPIE **8965**, 89650C (2014).
21. S. Hengesbach, S. Klein, C. Holly, U. Witte, M. Traub, and D. Hoffmann, "Simultaneous frequency stabilization and high-power dense wavelength division multiplexing (HP-DWDM) using an external cavity based on Volume Bragg Gratings(VBGs)," Proc. SPIE **9733**, 97330K (2016).

1. Introduction

Diode laser sources, with distinct advantages such as high electro-optical (E-O) efficiency and small volume, have extended the range of applications. However, due to the current limited brightness, diode laser sources are not suitable for many applications such as laser cutting. How to improve the brightness is a key technology problem to be solved [1–3]. The output power and brightness of diode laser sources can be increased through optimizing the design of diode emitters, such as minimizing divergence and improving power from a given aperture size, as well as through optical stacking and spectral multiplexing [4,5]. Over the last decade, several companies and research groups have explored novel beam multiplexing structures. Trumpf reported a diode laser source with an output power of 4 kW through wavelength beam combining (WBC). The beam quality is approximately 8 mm·mrad [6]. TeraDiode used WBC to develop a diode laser source with a power of 4680 W from an output fiber with a core diameter of 100 µm and a numerical aperture (NA) of less than 0.08. The fiber-coupled output corresponds to a beam quality of 3.5 mm·mrad [7]. In addition to WBC, dense spectral multiplexing (DSM) is an effective method for increasing brightness. DirectPhotonics obtained an output power of 450 W diode laser source with a beam quality of 4.5 mm·mrad by DSM [8]. The output power can be focused into a fiber with a core diameter of 100 µm and NA of 0.15. In this diode laser source, dichroic mirrors have been used to multiplex four wavelength channels within 12 nm. Fraunhofer ILT reported a fiber-coupled diode laser source with a power level of 800 W from an output fiber with a core diameter of 100 µm and NA of 0.17 [9], corresponding to a beam quality of 8.5 mm·mrad. Ultra-steep dielectric filters have been applied to realize dense spectral multiplexing. Because of the state of the art coating technology, commercial DSM based on dichroic mirrors and ultra-steep dielectric filters demands a spacing of ≥ 4 nm between adjacent wavelength channels, except for one research result achieving 2.5 nm [10], which results in a limited number of channels at a given spectral width (Table 1).

Table 1. State of the art commercial diode laser sources based on DSM technology. The data is given without any claim to completeness.

Institution	Multiplexing element	Channel spacing	Channel Wavelength	Beam quality	Effective bandwidth [1]	Maximum wavelength number
DirectPhotonics	Dichroic mirror	$\Delta\lambda = 4$ nm	943/947/951/955 nm	4.2 mm·mrad	30 nm	8
Fraunhofer ILT	Ultra-steep dielectric filters	$\Delta\lambda = 4$ nm	935.9/940.1/944.0 nm & 972.5/976.5/979.7 nm	8.5 mm·mrad	30 nm	8

[1]Usually, in coarse spectral multiplexing, each wavelength has an effective bandwidth of approximately 30 nm.

Highly dispersive reflective volume Bragg grating (VBG) in a photo–thermo–refractive (PTR) glass exhibits excellent spectral and angular selectivity. The maturation of manufacturing technology of VBGs has enabled the multiplexing of laser radiation from multiple wavelength channels with a spacing of 1.5 nm. The use of VBGs in DSM will increase the number of channels at a given spectral width. Hengesbach et al. reported a multiplexing system with a channel spacing of 1.5 nm and an optical power of 25.7 W [11]. To the best of our knowledge, the use of VBGs to develop a kW-class high power diode laser source with such narrow channel spacing has not yet been reported.

In this paper, we present a novel technology that uses reflective VBGs to multiplex laser radiation from five wavelength channels with the spacing of 1.5 nm. With the combination of polarization multiplexing and coarse spectral multiplexing (CSM), the diode laser source producing 2045 W power is realized. The beam quality of the laser source amounts to 4.5 mm·mrad which is suitable for coupling into a fiber with a core diameter of 105 μm and NA of 0.2. Experimental results show the ability of DSM based on VBGs to realize high output power and brightness.

A promising approach based on chirped DFB or DBR diode laser emitters is developed to realize DSM with a wavelength channel spacing of 1.5 nm [12]. In this approach, however, the integration of DFB or DBR structures into diode chip require a specific wafer runs for each wavelength [8]. By contrast, our present approach has no such requirement.

2. Optical stacking and spectral modulation

2.1 Optical stacking

The optical stacking of multiple diode laser single emitters is an efficient approach for power scaling [13,14]. The structural parameters of single emitters are shown in Table 2. The beam parameter product (BPP) is used to evaluate the beam quality of diode lasers and is defined as:

$$BPP = d_0 / 2 \cdot \theta_0 \tag{1}$$

where d_0 is the beam waist diameter and θ_0 is the half far field divergence [15]. Beam qualities of 0.37 mm·mrad in FA and 3.7 mm·mrad in SA, respectively, are obtained through Eq. (1). An optical structure based on a commercial building block is employed in this experiment. Nine single emitters with the same wavelength are mounted to a common staircase-like heatsink through a reflow soldering process. First the divergent output is collimated using FA collimation lenses, followed by SA collimation lenses. Correspondingly, nine reflective mirrors are integrated to stack the collimated beam geometrically in the FA direction. The spectrum of the whole building block under free running is illustrated in Fig. 1 with the 914.5 nm channel as an example.

Table 2. Structural parameters of single emitters in the laser source.

Parameter	Values
Chip width	500 μm
Emitter width	95 μm
Fast axis waist diameter	1.5 μm
Cavity length	4 mm
Center wavelength	91x nm/94x nm/97x nm
Output power @ 10 A (2% front facet reflectance)	10 W
θfast (95% power content)	56°
θslow (95% power content)	9°
E-O efficiency	55%
Mounting type	COS

Optics EXPRESS

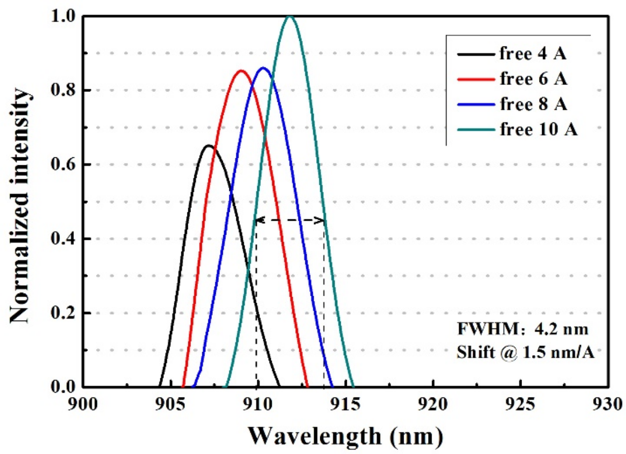

Fig. 1. Spectrum of the 914.5 nm building block under different injection current.

2.2 Spectral modulation

A narrow and stable spectrum is required for the subsequent DSM of diode laser building blocks with different wavelength channels. Thus, VBGs are employed to narrow and stabilize the spectrum. Given that the Bragg condition is related only to narrow deviation angles, the VBGs are located in the collimated beam. Spectrally narrow feedback from the VBGs is then imaged back on the front facet of the single emitters. The spectral width and locking range of the spectrum mainly depend on the reflectance of VBGs and the front facet. Figure 2(a) presents a three-dimensional cross-section laser model of the transverse electrical, thermal, and optical fields with attached external resonators for transverse and longitudinal mode selection. The model is generated using Crosslight software [16]. Multi-lateral modes and the corresponding photon densities are generated by solving the wave equation. The motion equation for the carriers inside the active region is used in reference to the unipolar electrical model. Poisson's equation describes the potential charge relation in a semiconductor with heterojunctions. The time-dependent photon rate equation is solved to relate optical power with modal gain and recombination. The k·p theory is used in strained quantum wells to obtain the accurate carrier concentrations and optical gain. These characteristics are dependent on the operation current. The characteristics of the external cavity are mainly calculated with the equivalent model. The optical parameters of the equivalent output facet are set to be the same as those of VBG. Figure 2 shows the numerical calculation results provided by Crosslight software. Reflectances of the front facet of single emitters are changed from 0.5% to 5%. And the reflectances of VBG are set to 10%, 15%, and 20%, respectively. Then the output power of the above external cavity is calculated when the single emitter operated at a current of 10 A. For the front facet of single emitters with Rf = 0.5…5%, the overall output power decreases as R_{VBG} increases. The R_{VBG} and R_f are set to 15% and 0.5%, respectively, in consideration of output power and spectral width.

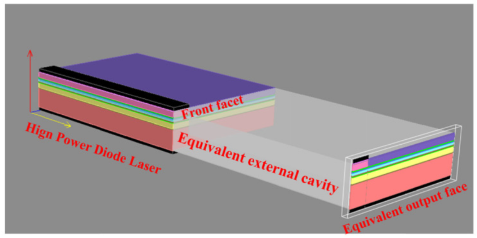

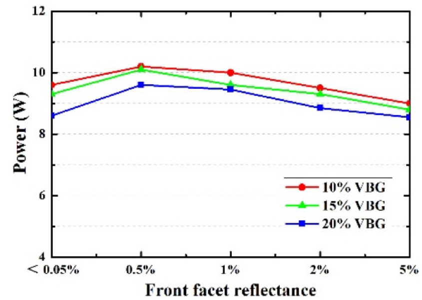

(a) (b)

Fig. 2. Optical output power per emitter (CW 25°C) at an injection current of 10 A as a function of front facet reflectance for different VBG reflectance.

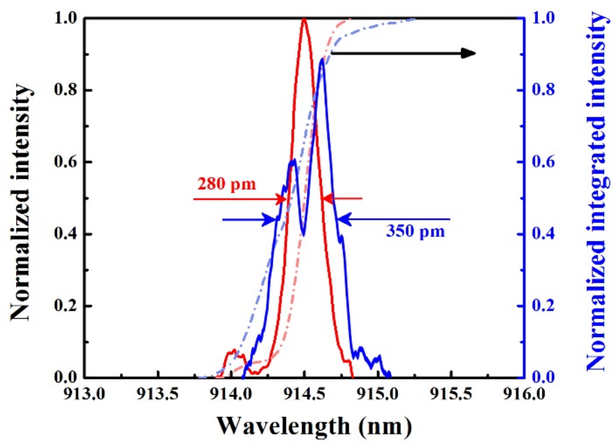

Fig. 3. Normalized spectral intensity and norm. Integrated intensity of single emitters with the center wavelength of 914.5 nm at I = 10 A.

However, side modes in the spectrum always occur and increase the spectral width. The occurrence of side modes is mainly due to the mismatch between the gain peak of the free running emitters and the Bragg-wavelength of VBGs [17]. Typically, to decrease this effect, the temperature of water coolant is adapted for each building block to match the Bragg-wavelength of VBGs [9]. However, this method would result in unsatisfactory heat dissipation and degrade the laser source lifetime [18]. Furthermore, side modes will continue to exist at high injection currents. We use the method in [9] to demonstrate this phenomenon and the spectral intensity of single emitters is plotted in Fig. 3 (blue line). As shown in Fig. 3, the spectral width is 350 pm (FWHM) which is broadened by the occurrence of side modes at 10 A. In our case, we select the desired single emitters from the epitaxial wafer to match the Bragg-wavelength of VBGs under free running. The single emitters operate at a narrow-band spectral intensity distribution with approximately 280 pm (FWHM), which significantly benefits from the side-mode suppression (red line).

3. Optical design of the multiplexing

3.1 Dense spectral multiplexing

In DSM, the spacing of adjacent wavelength channels is minimized to fully improve power and brightness. A DSM prototype of five wavelength channels with a spacing of 1.5 nm is presented in this work. Reflective VBGs are employed, and the wavelength channels are 913, 914.5, 916, 917.5 and 919 nm in 91x nm diode laser module. The optical design of the 91x nm diode laser module spectrally multiplexed by VBGs is shown in Fig. 4. The VBGs are fine tuned to match the Bragg condition of the respective wavelength channel for simultaneous reflection of a given channel and transmission of preceding channels. Moreover, the angular adjustment tolerance of the components is <0.05° [19]. Four VBGs are equal, so that the Bragg angles of the VBGs are different for each wavelength channel, the Bragg diffraction equation as below:

$$\left|\cos\theta_0\right| = \frac{\lambda}{2\Lambda n_{av}} \tag{2}$$

where θ_0 is the Bragg angle in VBG, λ is the wavelength of incident beam, Λ is the grating period and n_{av} is the average refractive index. In Eq. (2), the angles of incidence of the five wavelength channels are set as 25.377°, 25.178°, 24.977°, 24.775° and 24.572°.

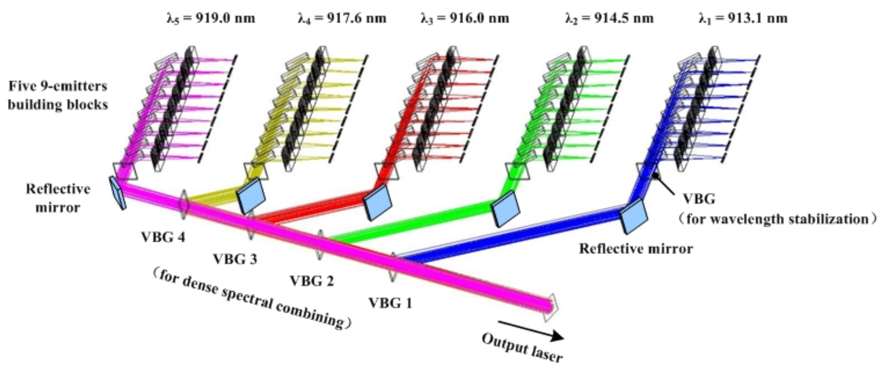

Fig. 4. Optical design of diode laser module operating at 91x nm based on dense spectral multiplexing.

From Fig. 4 we can see that the power irradiating on each VBG varies and the VBG 1 sustains the highest power. Given that the temperature dependent Bragg wavelength shift of VBGs is approximately 10 pm/K [20], the temperature difference caused by laser radiation may lead to a wavelength shift from 100 pm to 300 pm. Hence, controlling the temperature of reflective VBGs in DSM is necessary. In this work, water-cooled VBG holders are designed, and the flowing water coolant can efficiently remove heat of VBG. Four temperature sensors are laterally attached to the VBGs. By measuring the working temperature of VBGs, the temperature difference is controlled in a range of 5 °C. This approach almost eliminates the influence of temperature on the efficiency of multiplexing.

Similar results are obtained with two diode laser modules lasing at 94x and 97x nm. All wavelength channels are listed in Table 3.

Table 3. Stable wavelength channels of three diode laser modules.

	Channel 1	Channel 2	Channel 3	Channel 4	Channel 5
Module 1 (91x nm)	913.1	914.5	916.0	917.6	919.0
Module 2 (94x nm)	941.3	942.7	944.4	945.8	947.3
Module 3 (97x nm)	972.8	974.5	976.1	977.5	979.0

After DSM, the laser beam is polarization multiplexed to double power and brightness at a constant beam quality. The polarization coupler consists of a polarization beam splitter and a half waveplate. Transmittance and reflectance depend strongly on the polarization state of

Optics EXPRESS

laser radiation. We adjust the polarization state of laser radiation using the half wave plate. The beams of two diode laser modules with perpendicular polarization state are multiplexed when they reach the polarization beam splitter.

3.2 Coarse spectral multiplexing

CSM is utilized to multiplex three different wavelength modules with dichroic filters. The principle of CSM is to place precisely the transition region edge of dichroic filters between two wavelength channels for power scaling. Figure 5 shows the structural diagram of polarization multiplexing and CSM. First, 91x and 94x nm modules are multiplexed by dichroic filter 1 (91x nm R/94x nm T). Then, the radiation composed by 91x and 94x nm wavelengths beams are subsequently multiplexed with 97x nm beam by dichroic filter 2 (94x nm R/97x nm T).

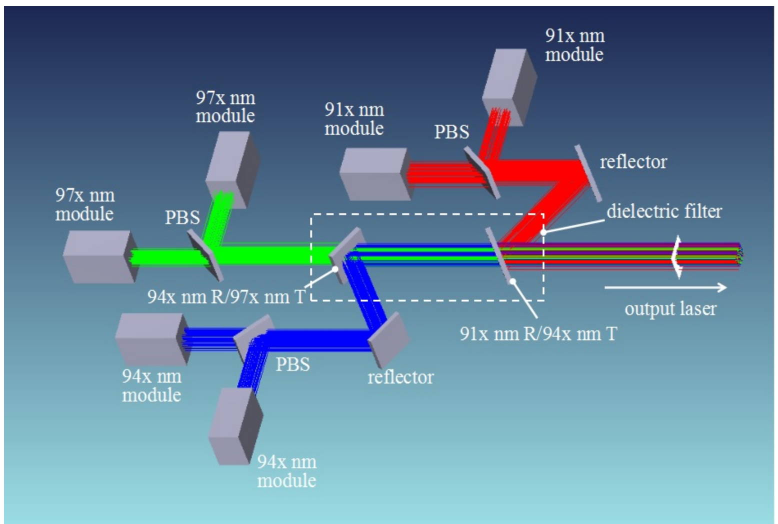

Fig. 5. Structural diagram of CSM.

We use a PerkinElemer Lambda-1050 spectrophotometer with a reflectance resolution of 0.1% to measure the spectral reflectance of dichroic filter. The measured reflectance curves of dichroic filters and spectral intensity of each module are plotted in Fig. 6. Because of the state of art coating technology, the transmittance to the long wavelength and reflectance to short wavelength of the dichroic filters are approximately 96% and 99%, respectively, which would cause power loss in CSM. In contrast to the spectral intensity with a spacing of 4 nm [8], we can see that an effective bandwidth of 30 nm exists between two filters for the 94x nm wavelength channel. This bandwidth provides sufficient space for the multiplexing of additional channels.

Optics EXPRESS

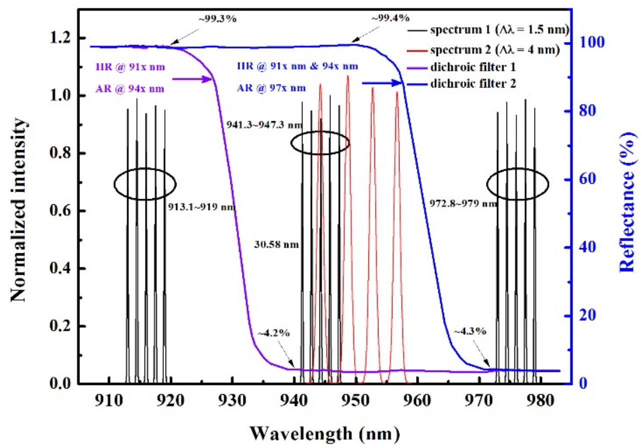

Fig. 6. Reflectance of the dichroic filters used in CSM. The spectral intensity distribution (black line) is stabilized with a spacing of 1.5 nm. For comparison, the spectral intensity distribution (red line) in [8] is plotted in the diagram.

4. Experimental results and analysis

At the coolant temperature of 25 °C and CW operating mode, the beam quality of 4.5 mm·mrad in the collimated beam after polarization multiplexing and CSM is measured by Primes focus monitor at 10 A, as shown in Fig. 7. Subsequently, an aspherical lens is employed to couple the output beam into a commercially available QBH fiber with a core diameter of 105 μm and NA of 0.2. The surfaces of the aspherical lens are covered with antireflective films with a transmittance of 99.7%. The power content in the far field of the beam after exiting the fiber as a function of NA is shown in Fig. 8. The NA exiting fiber is 0.16 for 95% power content.

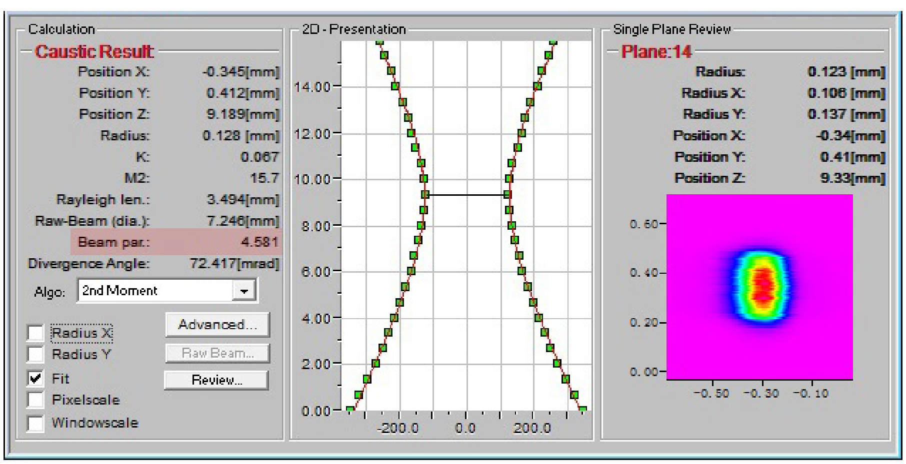

Fig. 7. Screenshot of the beam quality (mm·mrad) measurement using Primes focus monitor at I = 10 A.

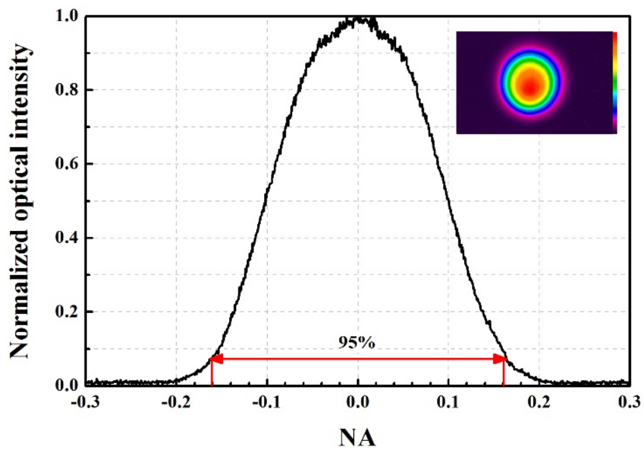

Fig. 8. The power content in the far field of the beam after exiting the fiber as a function of NA.

A CW power of 2045 W and an E-O efficiency of 42% are measured at the injection current of 10 A (Fig. 9). Nonetheless, the final optical-optical (O-O) efficiency of this diode laser source is limited to 76%, which is defined as the ratio of the multiplexing output power to the total free running power at 10 A. The output power and beam quality of each step is shown in Table 4. The main loss mechanism can be explained as follows:

The step of collimation and stacking experiences a power loss of approximately 5%. Surfaces of the FA and SA collimation lenses are covered by antireflective films with a residual reflectance of 0.3%. The accumulation of small imperfections in the coating leads to a relatively large power loss of 1.5% in total. To maximize filling density in optical stacking, the marginal rays of the collimated beam are cut by the reflective mirrors, which results in a loss of approximately 3.5%.

In DSM, the efficiency η_{MP} is defined as

$$\eta_{MP} = \frac{P_{MP}}{\sum P_{module,i}} \quad (3)$$

with the power $P_{Module,i}$ emitted by module i and the power P_{MP} in the dense spectral multiplexed beam. A multiplexing efficiency of approximately 93% at the operating point of 10 A is achieved for the modules at 91x, 94x and 97x nm.

In polarization multiplexing, the efficiency of polarization amounts to 96%, which is defined as the ratio of the power measured behind the polarization coupler to the power measured before the coupler. The single emitters used in this work have a degree of polarization of 98%, which also cause the power loss in polarization multiplexing.

In CSM, efficiency is defined as the ratio of the power measured behind the polarization coupler to the power measured behind the dichroic filter. Hence, the transmittance to the long wavelength and reflectance to the short wavelength of the dichroic filters are approximately 96% and 99%, respectively.

A fiber coupling efficiency of approximately 93.6% at the operating point of 10 A is obtained. The efficiency η_{FC} is defined as

$$\eta_{FC} = \frac{P_{ex100\mu m}}{P_{beh,CWM}} \quad (4)$$

where the $P_{ex100\mu m}$ is the output power from the fiber, and $P_{beh,CWM}$ is the power after CSM. The power before entering the fiber and after exiting the fiber as a function of current are shown in Fig. 9. Coupling efficiency is limited by the reflection loss of aspherical lens and the overfilling of the clear aperture of the fiber core.

Table 4. Power measured after each step under I = 10 A.

Step	Power (W)			Efficiency	BPP (mm·mrad)
	91x nm	94x nm	97x nm		
Collimation & stacking	84.6	85.5	86.8	95%	3.9
DSM	391.4	397.6	403.6	93%	/
Polarization multiplexing	753.3	763.4	774.9	96%	/
CSM		2184		R99%/T96%	4.5
Fiber coupling		2045		93.6%	5.5

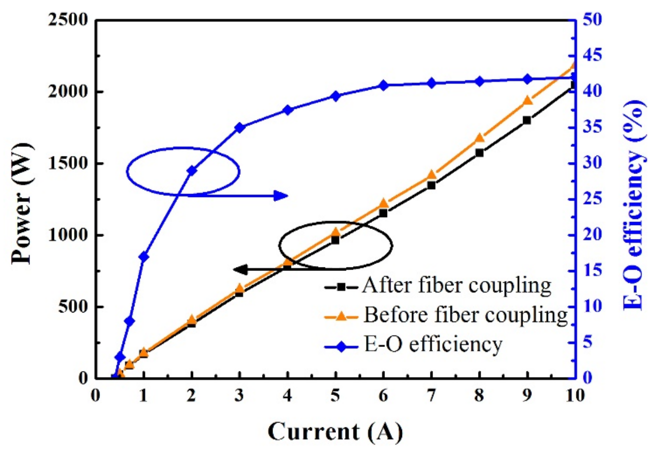

Fig. 9. Output power and E-O efficiency as a function of injection current.

Fraunhofer ILT also presented a multiplexing structure with an average channel spacing of 1.7 nm and a subsequent external cavity mirror to provide feedback for frequency stabilization and multiplexing in one step [21]. This method is simpler than our method, but it requires a higher adjustment accuracy and the stabilization of all optical elements. In contrast to WBC, our method is based on the commercial building blocks, which can increase stabilization and decrease manufacture costs.

5. Summary and conclusion

We demonstrate a novel structure for power scaling in this paper. Reflective VBGs are used for the DSM of five wavelength stabilization channels with a spacing of 1.5 nm. Through the combination of polarization multiplexing and CSM, a CW power of 2045 W from an output fiber with a diameter of 105 µm and NA of 0.2, an E-O efficiency of 42% and an O-O efficiency of 76% are obtained. This work demonstrates the ability of VBG-based DSM to realize high output power and brightness.

Funding

National Natural Science Foundation of China (NSFC) (61674149).

Acknowledgments

We thank our project partners for the assistance and fruitful discussions.